IJRAR.ORG E-ISSN: 2348-1269, P-ISSN: 2349-5138

INTERNATIONAL JOURNAL OF RESEARCH AND ANALYTICAL REVIEWS (IJRAR) | IJRAR.ORG

An International Open Access, Peer-reviewed, Refereed Journal

SYNTHESIS AND CHARACTERIZATION OF PVDF-DES BASED ETHANOL SENSOR

[1]Pratibha Yadav, [2]Kamlesh Pandey, [2]Mrigank Mauli Dwivedi, [3]Saurabh Kumar Tiwari, [1]Sharda Sundaram Sanjay

[1]Department of Chemistry, Ewing Christian College, Prayagraj-211002, India

[2]National Center of Experimental Mineralogy and Petrology, University of Allahabad, Prayagraj-211002, India

[3]Department of Chemistry, K.B.P.G. College, Mirzapur, U.P., India

Abstract: The polymer membranes (80PVDF-20DES) and $(80PVDF\text{-}20DES)_{0.95}$:$BAG_{0.05}$ were synthesized and characterized through different experimental techniques. The structural behavior of the polymer composite membrane is investigated by XRD and FTIR. XRD curve revealed the amorphous nature of the membrane. The use of BAG as filler in composites provided a better polymer interface as well as the high free volume size, through which molecule transport occurs in polymer-composite membrane matrix. The polymer glass composite membrane shows high porosity which becomes a major responsive factor to enhance the ionic conductivity. It is also favorable for better conduction and sensing behavior for ethanol sensor.

1. INTRODUCTION

In recent years, polymer-based gas sensors have garnered considerable interest owing to their inherent flexibility, lightweight nature, cost-effectiveness, and capability to function efficiently at room temperature[1–5]. Among these, polyvinylidene fluoride (PVDF) stands out as a highly promising sensing material due to its excellent thermal stability, mechanical robustness, and pronounced dipolar characteristics[6–8]. The integration of deep eutectic solvents (DES) into the PVDF matrix has been shown to significantly enhance ionic mobility and surface polarity, thereby improving gas-sensing performance. Further advancement is achieved by incorporating bioactive glass (BAG) into the PVDF–DES composite. BAG[9,10], comprising both network-forming and network-modifying oxides, contributes to increased surface roughness, a higher density of active sites, and enhanced interfacial interactions within the polymer matrix[11–13]. These features collectively facilitate more efficient charge transport pathways, leading to a heightened sensor response.

In the present study, a DES formulated from urea and glycerol was synthesized and evaluated for its suitability in polymer film fabrication and gas-sensing applications, with a particular focus on ethanol vapour detection[14,15]. The resulting PVDF–DES–BAG composite is anticipated to exhibit superior gas-sensing characteristics due to its improved surface activity, elevated polarity, and optimized charge transport mechanisms. To substantiate these enhancements, the composite was thoroughly characterized using X-ray diffraction (XRD), Fourier-transform infrared spectroscopy (FTIR), Raman spectroscopy, scanning electron microscopy (SEM), and ionic conductivity measurements.

2. EXPERIMENTAL

Materials used for the Synthesis of Polymer-DES Films with Bioactive Glass (BAG) Filler of DES were; Polyvinylidene fluoride (PVDF)[Alfa Asar], N,N-Dimethylformamide (DMF)[SRL] ,Double distilled water, Urea [Rankem], Glycerol[Merck] and self-fabricated Bioactive glass (BAG 45S5). The composition of bioactive glass is 45% SiO_2, 24.5% Na_2O, 24.5% CaO, and 6% P_2O_5. This glass is synthesized by sol gel technique[16].

The deep eutectic solvent (DES) used in this study was synthesized by mixing urea and glycerol in a 2:1 molar ratio. The mixture was stirred continuously at 80 °C for 1 hour using a magnetic stirrer. A thick transparent and homogeneous liquid was obtained, indicating the successful formation of the DES through hydrogen bonding interactions between urea and glycerol.

Polymer films were prepared using polymers: polyvinylidene fluoride (PVDF), dissolved in dimethylformamide (DMF) at 70 °C The solutions were stirred for 2 hours at 50 °C temperature to ensure complete dissolution of the polymers. After this, the prepared DES was added separately to polymer solution. The ratio of polymer to DES was maintained at 80:20 (w/w) for film formulations. The mixtures were stirred thoroughly for 2-3 hours. The final mixtures poured into plastic petri dishes and dried at controlled temperatures. The synthesized membrane (80PVDF-20DES) and $(80PVDF\text{-}20DES)_{0.95}$:$BAG_{0.05}$ is used for the alcohol (ethanol) sensor. Structural behaviour of composite polymer electrolyte membranes were carried out by X-ray diffractometer (Philips X-Pert model) in the 2θ range (10° to 70°). The SEM images of different electrolyte systems were recorded with the JEOL JXA-8100 EPMA instrument. For SEM imaging the polymeric membranes (size ~ 2mm x 2mm) were fixed on a stub with the help of double sided carbon tape and Carbon coating (~10-15nm) was done on the membranes using Jeol vacuum evaporator JEE-420. Infrared spectroscopic measurements were carried out on a Bruker Alfa (Germany) ATR -IR spectrophotometer in the range 4000 cm^{-1} – 600 cm^{-1} at room temperature. All the spectra were recorded at a resolution 4 cm^{-1} and with an accumulation of 8-32 scans.

3. Results and Discussion

The XRD pattern of (80PVDF-20DES) membrane given in Figure 1(A) exhibits some crystalline peaks at 2θ = 20.6° , 36.6° , 39.5°and 56.6°, characteristic of the β and α phases of PVDF the effect of two phases introduced after dissolution of PVDF in DES.

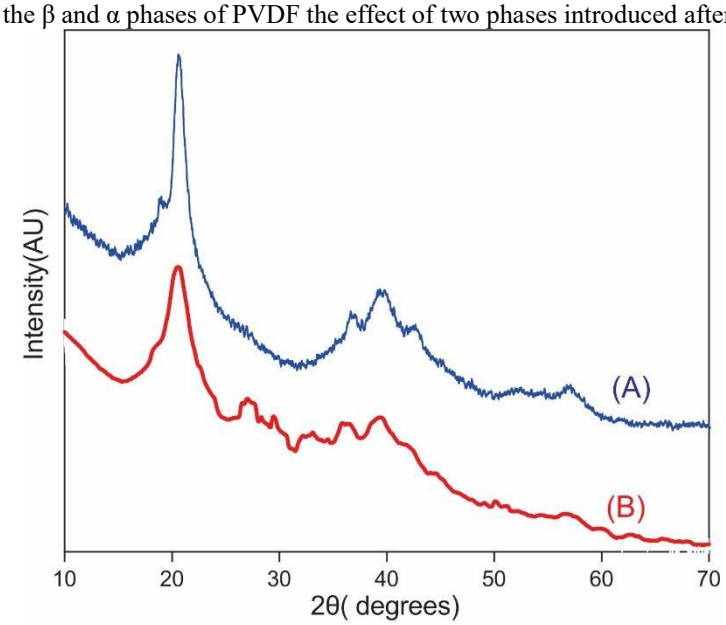

Figure 1: XRD pattern of (A) (80PVDF-20DES) membrane and (B) $(80PVDF\text{-}20DES)_{0.95}$:$BAG_{0.05}$ composite membrane.

These peaks with hollow base of XRD pattern also infers the semi crystalline nature of the (80PVDF-20DES) membrane. After the addition of BAG Figure 1(B) the intensity of 2θ = 20.6° peak reduces and the broadness of peak around 39.5° is slightly enhanced, which indicate the increase in amorphous nature of composite electrolyte.

The FTIR spectra of (80PVDF-20DES) & (80PVDF-20DES)0.95: BAG0.05 are shown in Figure 2 the assignments of main peaks are given in Table 1. In both membranes broad peak observed 3441 cm^{-1} assigned as N-H bonding supported by –OH stretching is due to the glycerol present in DES. After the incorporation of BAG in the polymer matrix it shifted lower side i.e. 3348 cm-1. This suggests the formation of hydrogen bonding between N-H/hydroxyl groups of the DES and (Si–OH) groups present in BAG.

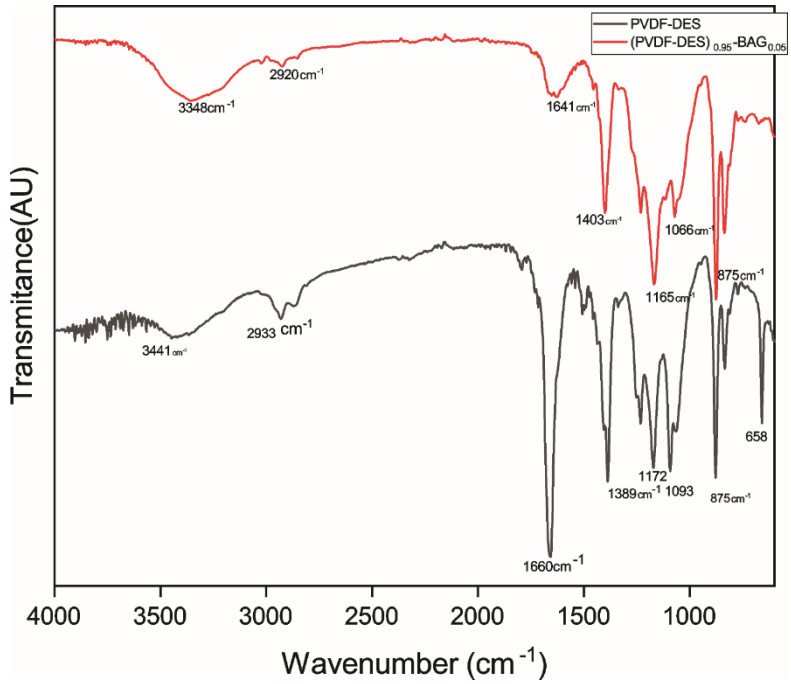

Figure 2: FTIR spectra of composite polymeric membranes.

Table 1: FTIR-main peaks and their assignments

PVDF-DES (cm^{-1})	PVDF-DES-BAG (cm^{-1})	Assignments of peak
3441 -	- 3348	O–H stretching
2933 -	- 2920	C–H stretching
1660 -	- 1641	C=C stretching / C=O interaction
- 1389	1403 -	CH_2 bending & asymmetric stretching CO_3^{2-}
1172 - 1093	- 1165- 1066	C–F stretching , Si–O–Si stretching
875	875	C–F bending , Si–O bending
658	-	CF_2 bending vibration

The C–H stretching vibration peak of glass originally at 2933 cm^{-1}, also shown a shift of 13cm^{-1} in the BAG-containing film, indicating interactions of glass with the polymer backbone. Similarly, a peak at 1660 cm^{-1}, i.e. C=C or C=O stretching, was observed in PVDF-DES goes to the lower side at 1641 cm^{-1} with low intensity in the BAG composite, possibly due to the interaction of unsaturated or polar functional groups and the glass phase. The peaks at 1389 cm^{-1} and 1403 cm^{-1} in the BAG composite were assigned to CH_2 bending and CO_3^{2-} asymmetric stretching, suggesting the presence of carbonate groups contributed by the glass composition. A prominent absorption peak observed 1172 cm^{-1} which assigned C-F stretching vibration of PVDF. This also shifted to 1655 cm^{-1} BAG composite. The C–F stretching and Si–O–Si overlapping vibration, originally at 1093 cm^{-1} in PVDF-DES, was replaced by a prominent peak at 1066 cm^{-1} in $(80PVDF\text{-}20DES)_{0.95}$:$BAG_{0.05}$. This shift confirms interaction between fluorinated segments of PVDF and the silica network of BAG. The C–F bending and Si–O bending vibrations remained consistent at 875 cm^{-1} in both films, indicating structural stability in that region. In (80PVDF-20DES), a band at 658 cm^{-1} corresponds to CF_2 bending vibration, which disappeared in $(80PVDF\text{-}20DES)_{0.95}$:$BAG_{0.05}$, due to BAG addition.

To analyze theoretically the molecular interactions in detail, the broad peak in range of 1500–1700 cm^{-1} were fitted for both (80PVDF-20DES) and $(80PVDF\text{-}20DES)_{0.95}$:$BAG_{0.05}$ films shown in Figure 3 and Figure 4. The (80PVDF-20DES) spectrum showed three sharp peaks at 1648, 1661, and 1663 cm^{-1}, which are attributed to C=O stretching vibrations, and the $(80PVDF\text{-}20DES)_{0.95}$:$BAG_{0.05}$ sample exhibited three broader peaks at 1548, 1636, and 1643cm^{-1}. The broadening of peaks in the BAG-incorporated film suggests increased molecular interactions, possibly due to hydrogen bonding and the presence of Si–OH group of glass. The peak at 1548 cm^{-1} may also indicate N–H bending, suggesting chemical interaction between the polymer matrix and the glass.

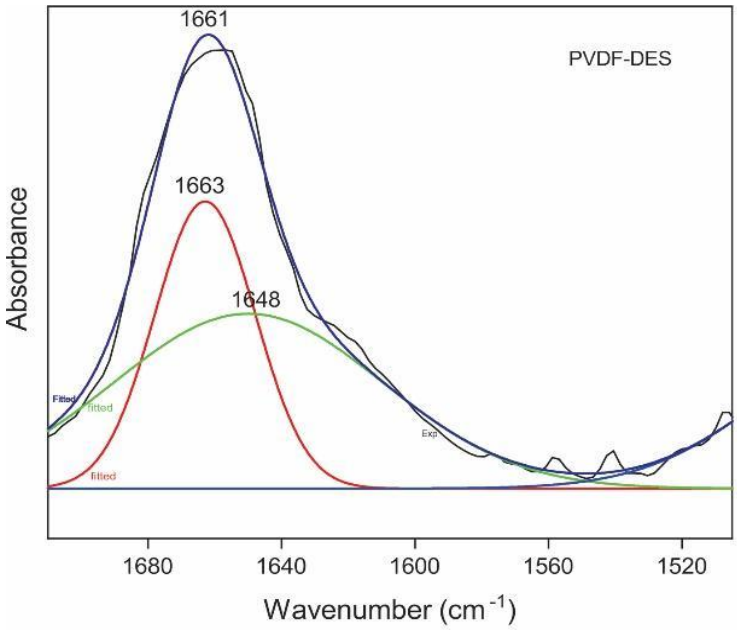

Figure 3: Deconvolution spectra of characteristic peak ~ 1670cm^{-1} in (80PVDF-20DES) membrane.

The Raman spectra of the (80PVDF-20DES) and $(80PVDF\text{-}20DES)_{0.95}$:$BAG_{0.05}$ film shown in Figure 5 exhibited a broad characteristic band at around 380 cm^{-1}, which is typically associated with the vibrational modes of the PVDF matrix. However, a significant change was observed after the incorporation of BAG into the (80PVDF-20DES) system the characteristic peak at the 380 cm^{-1} band, disappeared completely in the $(80PVDF\text{-}20DES)_{0.95}$:$BAG_{0.05}$ composite. This disappearance of peaks can be attributed to the strong scattering from BAG particles, the incorporation of BAG may introduce structural disturbance within the polymer network, resulting in a reduction of Raman activity.

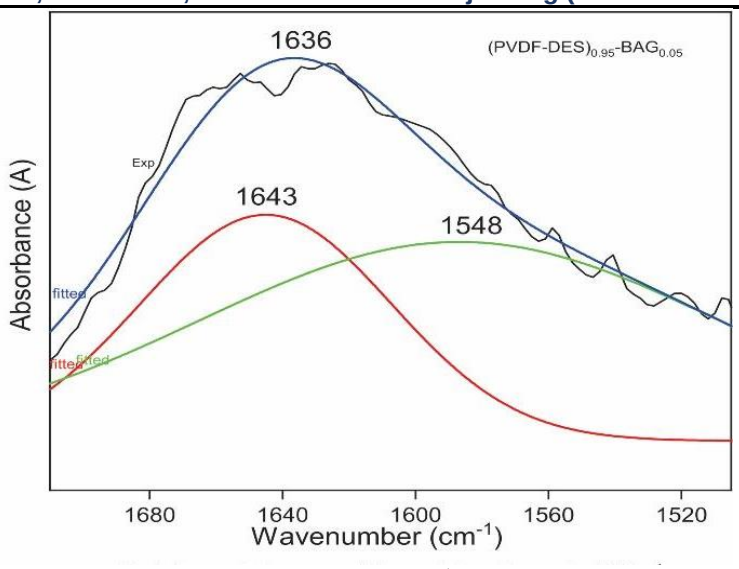

Figure 4: Deconvolution spectra of characteristic peak around ~ 1640cm^{-1} in (80PVDF-20DES)$_{0.95}$:BAG$_{0.05}$ composite membrane.

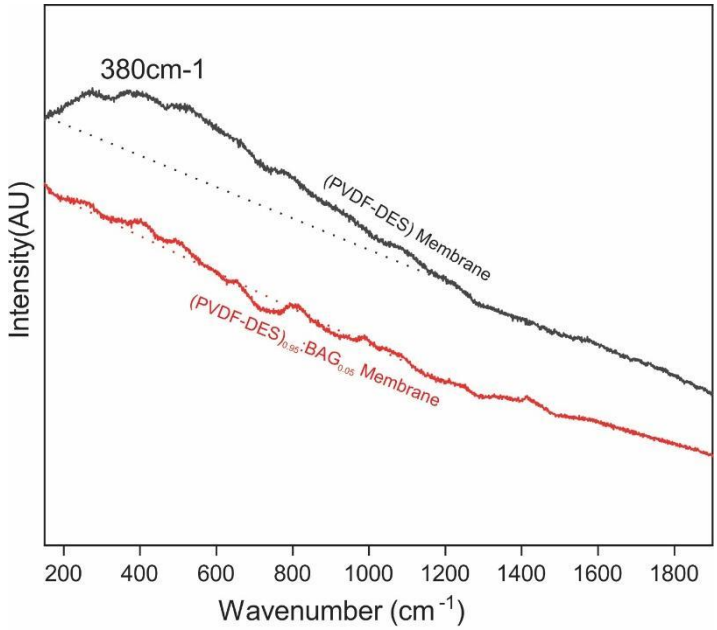

Figure 5: Raman spectra of (80PVDF-20DES) membrane and (80PVDF-20DES)$_{0.95}$:BAG$_{0.05}$ composite membrane.

The Scanning Electron Microscopy (SEM) image of the (80PVDF-20DES) and (80PVDF-20DES)$_{0.95}$:BAG$_{0.05}$ film shown in Figure 6. Figure 6(a) i.e. (80PVDF-20DES) film displays the presence of small pores distributed across the film surface. After the addition of BAG (Figure 6(b)) clearly shows the bigger pores which are more pronounced.

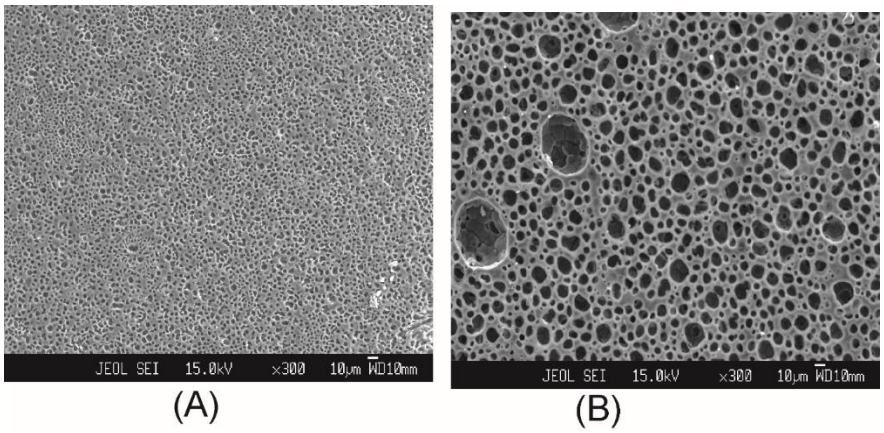

Figure 6 Scanning Electron Microscopy (SEM) image of the (80PVDF-20DES) and (80PVDF-20DES)$_{0.95}$:BAG$_{0.05}$ membrane.

This indicates that BAG incorporation affected the PVDF matrix leading to increased porosity. These observations suggest that the surface morphology is more sensitive to BAG incorporation in PVDF-based films.

The ionic conductivity values of (80PVDF-20DES) and (80PVDF-20DES)$_{0.95}$:BAG$_{0.05}$ were measured at different frequencies ranging from 100 Hz to 100 kHz. It was observed that the conductivity at low frequency almost equal in both membranes, indicating minimal effect of BAG. As frequency increases, the conductivity of both samples increases. At high frequency (80PVDF-20DES)$_{0.95}$:BAG$_{0.05}$ shows a slightly higher conductivity compared to (80PVDF-20DES) indicating that the addition of BAG enhances conductivity. The measured value of conductivity of with and without glass are given in Table 2.

Table 2: Conductivity of polymer membranes.

Frequency (Hz)	PVDF-DES Conductivity (S/cm)	PVDF-DES-BAG Conductivity (S/cm)
10E+05	1.35E-06	1.84E-06
10E+04	1.09E-07	1.74E-07
10E+03	1.12E-08	1.53E-08
10E+02	2.41E-09	2.48E-09

3.1. Application of Membrane

The synthesized membrane (80PVDF-20DES) and $(80PVDF\text{-}20DES)_{0.95}:BAG_{0.05}$ is used for the alcohol (ethanol) sensor. The experimental setup is shown in Figure 7 before the study of sensing behavior of the membrane we study the absorption of ethanol directly. Weight of membrane before and after soaking of ethanol is almost same but the change in conductivity of the ethanol soaked membrane is increased almost 100 time (i.e. 2.4E-9 S/cm to 2.4E-7 S/cm) This shows the sensing behavior of free membrane.

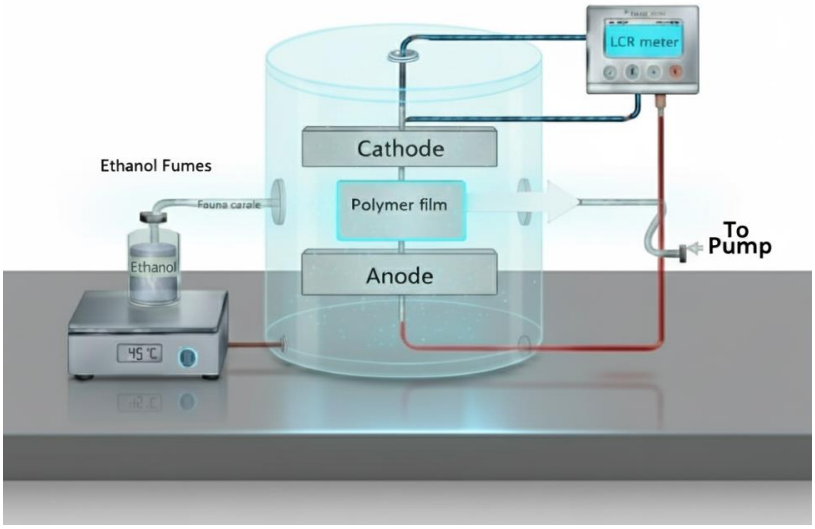

Figure 7 Experimental setup of conductometric Ethanol sensor.

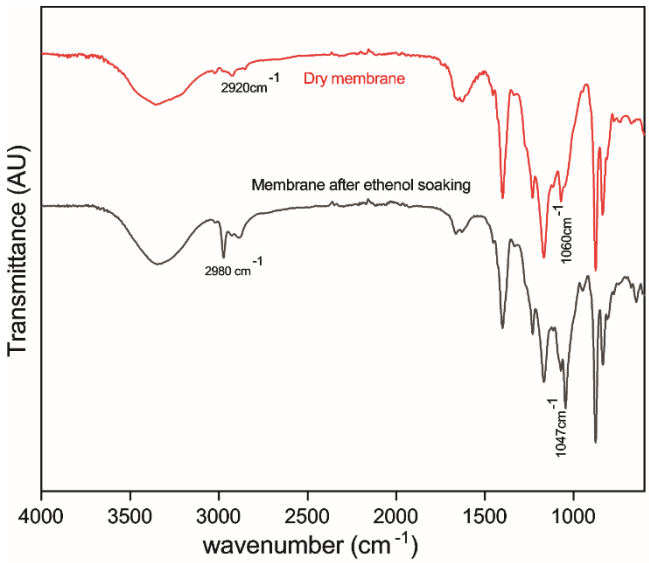

Figure 8 FTIR spectra of $(80PVDF\text{-}20DES)_{0.95}:BAG_{0.05}$ composite membrane before and after the absorption of ethanol.

To examine structural or chemical changes due to ethanol absorption to confirm the absorption/sensing of ethanol on both membranes we record the FTIR spectra before and after the absorption of ethanol and shown in Figure 8 and Figure 9**.** In the (80PVDF-20DES) dry film, peaks at 3335, 2917, 2355, and 1671 cm^{-1} were clearly present, but disappeared after absorption of ethanol, indicate strong ethanol interaction and alters the chemical environment of functional groups. In $(80PVDF\text{-}20DES)_{0.95}:BAG_{0.05}$, the dry film showed a C–H stretching peak at 2920 cm^{-1} and a Si–O / C–F related band near 1060 cm^{-1}, while after ethanol exposure the peaks shifted to 2980 cm^{-1} and 1047 cm^{-1}, respectively. This shift indicates structural rearrangement, weakening of $(80PVDF\text{-}20DES)_{0.95}:BAG_{0.05}$ interactions, and possible exposure of BAG silicate groups.

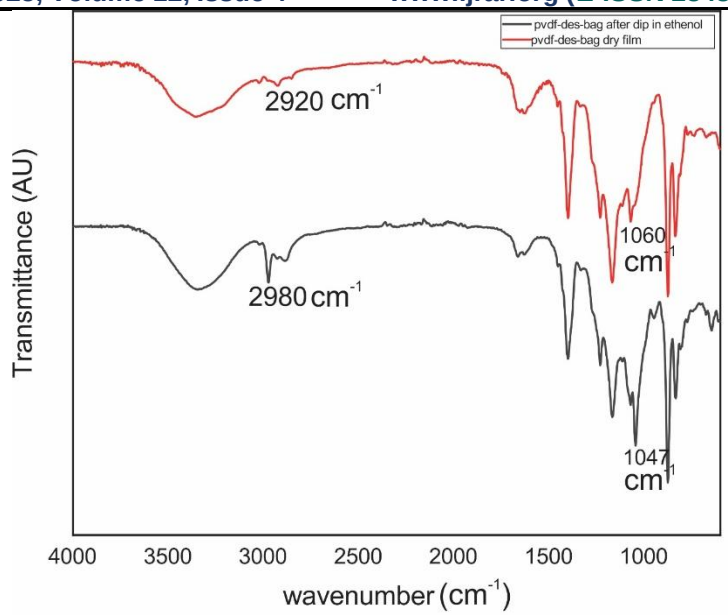

Figure 9 FTIR spectra of $(80PVDF\text{-}20DES)_{0.95}$:$BAG_{0.05}$ composite membrane before and after the absorption of ethanol.

Overall, the disappearance of some peaks and shifting of others clearly confirm that ethanol interacts with all the films, indicate that the fabricated polymer films are responsive towards ethanol, supporting their potential for ethanol sensing applications.

4. Conclusion

We have successfully developed urea-glycerol DES-based ethanol responsive polymer films. The surface morphology of PVDF-based films appears to be more sensitive to BAG inclusion, as evidenced by SEM figures as BAG incorporation altered the PVDF matrix, resulting in increased porosity. The ionic conductivities in both films have shown similar conductivities at lower frequencies but at higher frequencies, PVDF-DES-BAG film has shown greater conductivity. We have also observed increased surface area (ie 100 times) with better activity, eminent polarity, and optimized charge transport mechanisms. The increased conductivity in ethanol soaked PVDF-DES-BAG film, making this film a potent alcohol-sensor.

Acknowledgement: Authors are thankful to Prof. K. N.Uttam for providing the Laser Raman facility.

References

[1] AlTakroori, H. H. D., Ali, A., Greish, Y. E., Qamhieh, N. & Mahmoud, S. T. Organic/Inorganic-Based Flexible Membrane for a Room-Temperature Electronic Gas Sensor. *Nanomaterials* **12**, 2037 (2022).
[2] De, G., Karmakar, B. & Ganguli, D. Hydrolysis–condensation reactions of TEOS in the presence of acetic acid leading to the generation of glass-like silica microspheres in solution at room temperature. *J. Mater. Chem.* **10**, 2289–2293 (2000).
[3] Neri, G. First Fifty Years of Chemoresistive Gas Sensors. *Chemosensors* **3**, 1–20 (2015).
[4] Wen, J. *et al.* Recent progress in polyaniline-based chemiresistive flexible gas sensors: design, nanostructures, and composite materials. *J. Mater. Chem. A* **12**, 6190–6210 (2024).
[5] Yan, Y. *et al.* Conducting polymer-inorganic nanocomposite-based gas sensors: a review. *Science and Technology of Advanced Materials* **21**, 768–786 (2020).
[6] Dallaev, R. *et al.* Brief Review of PVDF Properties and Applications Potential. *Polymers* **14**, 4793 (2022).
[7] Mohammadpourfazeli, S. *et al.* Future prospects and recent developments of polyvinylidene fluoride (PVDF) piezoelectric polymer; fabrication methods, structure, and electro-mechanical properties. *RSC Adv.* **13**, 370–387 (2023).
[8] Srinivasaraghavan Govindarajan, R. *et al.* Polymer Nanocomposite Sensors with Improved Piezoelectric Properties through Additive Manufacturing. *Sensors* **24**, 2694 (2024).
[9] Hench, L. L. The story of Bioglass®. *J Mater Sci: Mater Med* **17**, 967–978 (2006).
[10] Mohn, D. *et al.* Composites made of flame-sprayed bioactive glass 45S5 and polymers: bioactivity and immediate sealing properties. *Int Endodontic J* **43**, 1037–1046 (2010).
[11] Sekhon, S. Solvent effect on gel electrolytes containing lithium salts. *Solid State Ionics* **136–137**, 1189–1192 (2000).
[12] Sergi, R., Bellucci, D. & Cannillo, V. A Review of Bioactive Glass/Natural Polymer Composites: State of the Art. *Materials* **13**, 5560 (2020).
[13] Shuai, C. *et al.* Tailoring properties of porous Poly (vinylidene fluoride) scaffold through nano-sized 58s bioactive glass. *Journal of Biomaterials Science, Polymer Edition* **27**, 97–109 (2016).
[14] Abbott, A. P., Boothby, D., Capper, G., Davies, D. L. & Rasheed, R. K. Deep Eutectic Solvents Formed between Choline Chloride and Carboxylic Acids: Versatile Alternatives to Ionic Liquids. *J. Am. Chem. Soc.* **126**, 9142–9147 (2004).
[15] Zdanowicz, M. & Sałasińska, K. Characterization of Thermoplastic Starch Plasticized with Ternary Urea-Polyols Deep Eutectic Solvent with Two Selected Fillers: Microcrystalline Cellulose and Montmorillonite. *Polymers* **15**, 972 (2023).
[16] Sanjay, S. S., Yadav, P., Asthana, N., Dwivedi, M. M. & Pandey, K. An investigation on 45S5 nanobioactive glass using FTIR and Raman spectroscopy. *Charact. Appl. Nanomater.* **6**, 4152 (2023).